JOURNAL OF MATERIALS SCIENCE 29 (1994) 1553–1557

Broadened X-ray-diffraction profile analysis of cold-rolled aluminium–magnesium alloys

N. JI, J. L. LEBRUN
LMMM, UA CNRS 1219, ENSAM, 151 Bd. de l'Hôpital, 75013, Paris, France
P. SAINFORT
PECHINEY, Centre de Recherche, B.P. 27, 38340 Voreppe, France

A cold-rolled, commercial pure aluminium and three aluminium–magnesium alloys (containing, respectively, 1 wt%, 3 wt% and 5 wt% magnesium) were studied by X-ray-diffraction (XRD) profile analysis. The investigated equivalent plastic deformations of the materials were ranged between 0.1 and 5.0. With increases in the amounts of magnesium, the diffraction peaks widened. For each alloy, the peak width (which gives first information from the analysis) increased for low deformation ratios and reached a maximum value, ds_{max}, and then it decreased or stabilized. The ds_{max} value increased with increases in the amount of magnesium in the alloys and ranges for equivalent deformation $\bar{\varepsilon} = 0.3$ and 1.5. The results of the X-ray profile analysis have been correlated with previous observations by transmission electron microscopy (TEM), and they have been successfully used to quantify the microstructural features of the alloys.

1. Introduction

The development of dislocation substructures in materials and alloys during plastic deformation, and the corresponding mechanical properties evolution, are still of considerable interest from both a scientific and a practical point of view. Current models of strain–stress descriptions of solid solutions describe the hardening effect caused by the formation and the multiplication of crystallographic defects [1, 2]. These defects are either two-dimensional or linear. In the two-dimensional case the hardening effect is described by the conventional Hall–Petch law

$$\sigma(\varepsilon) = \sigma_0(\varepsilon) + K(\varepsilon)d^{-n} \qquad (1)$$

where d is the grain size or dislocation cell size. In the linear case the hardening effect is governed by dislocation distributions

$$\sigma(\varepsilon) = \alpha\mu \boldsymbol{b}/d = \alpha\mu \boldsymbol{b}\rho^{1/2} \qquad (2)$$

where d is the mean distance between the dislocations, $\boldsymbol{b}$ is the Burgers vector and ρ is the dislocation density (α is a constant equal to about 1/4 for a face-centred-cubic (f.c.c.) structure). These hardening mechanisms have been studied in order to explain the mechanical properties of pure aluminium and aluminium–magnesium alloys [2–5]. Beside their practical interest, the aluminium–magnesium alloys are solid solutions (for magnesium contents below 17.4 wt % at 450 °C); and the magnesium atoms of large radius are in substitutional positions in the aluminium f.c.c. lattice, leading to a considerable elastic distortion of the crystalline lattice, which modifies the dislocation mobility and the alloys plastic deformation behaviour.

An improved understanding of the deformation modes for polycrystalline materials therefore requires statistical information about the dislocation substructures. These are, however, mainly studied by direct methods, such as observation by optical microscopy or transmission electron microscopy (TEM). TEM analysis allows direct observation of microstructural features (grain boundaries, dislocation cells, etc.) but at a very local scale of the volume studied, and care must be taken with thin-foil preparations and their interpretation as far as problems such as relaxation effects or dislocation surface interactions are concerned [3–6].

The X-ray-diffraction (XRD) method is of particular interest as a complement to TEM, since it provides reliable information especially for high dislocation densities, which are not easily investigated by the TEM technique [4–6]. As a matter of fact, the XRD method is non-destructive and it allows the investigation of *macroscopic volumes* in bulk material. For instance, XRD peak broadening can be observed when the material has been cold worked. This effect can be used to interpret the deformation microstructural evolution of materials [7–8], and it has been developed theoretically and experimentally to a considerable extent recently [8–10]. The microstructure-evolution results were accurately correlated with TEM observations [11, 12].

The aim of this study was to tentatively correlate and explain the evolution of XRD profile broadening of different aluminium alloys in relation to their work hardening and dislocation substructure.

Commercial pure aluminium and three aluminium–magnesium solid solutions were studied in this

0022–2461 © *1994 Chapman & Hall*

work. The alloys have been characterized elsewhere by TEM, and also by mechanical tests in [13, 14].

2. Materials and experimental procedure

The chemical compositions of the commercial pure aluminium and the three aluminium–magnesium alloys (1 wt % Mg, 3 wt % Mg and 5 wt % Mg) used in this study are given in Table I. Homogenization heat treatments were performed at 420 °C for 16 h under a dry argon atmosphere. The aluminium–magnesium alloys were quenched in water in order to stabilize the solid solutions. The treated samples (in the form of sheets) were then cold rolled. The final equivalent plastic-deformation ratio, $\bar{\varepsilon}$, was varied from 0.10 to 5.0.

XRD profiles were recorded on a SEIFERT-TS goniometer with a position-sensitive detector. The reflection planes selected for the study were $\{1\,1\,1\}$ and $\{2\,2\,2\}$. A chromium tube and a vanadium filter were used in the experiments.

In order to avoid surface effects, the specimen surfaces were electrolytically polished to remove about 0.1 mm in depth. The counting time was optimized to minimize statistical errors (about 300 s for the $\{1\,1\,1\}$ reflection, and 600 s for the $\{2\,2\,2\}$ reflection leading to a total integral intensity of about 10000 counts s^{-1}). The error in the peak position was less than 0.005° and the uncertainty in the peak width was less than 5%. An annealed aluminium specimen was used as a reference (standard) diffraction peak for instrumental broadening corrections in a Fourier-analysis calculation.

A broadened-profile analysis was carried out in a way which was based on Warren–Averbach principles; this was developed recently in our laboratory [9] in order to calculate the integral peak width, ds, the average coherent domain size, D, and the distortion factor, ε_1 (or the mean square strain $\langle \varepsilon_L^2 \rangle$) from the recorded profiles of two orders of reflection (1 1 1 and 2 2 2 in this present study). Note that ds is a global indicator of the microstructural state of the material. D is the size, in the crystallographic direction investigated, of an equivalent three-dimensional perfect crystal which could be defined by the mean distance between crystallographic defects in the specimen. ε_1 is the average elastic distortion in coherent domains, in the investigated direction, and it results in the microscopical distortion induced by the defects around coherent domains. These parameters are used for a quantitative description of the crystallographic defect density and the distribution [10, 15]. In the case of plastic deformation, they are in close relationship with the dislocation density and distribution.

TABLE I The chemical compositions of the materials used in the study

	Compositions (p.p.m.)				
	Mg[a]	Fe	Cu	Zn	Si
Commercial Al	20	17	45	–	20
Al–1% Mg	1 ± 0.03%	22	36	28	< 500
Al–3% Mg	3.1 ± 0.1%	26	28	71	< 500
Al–5% Mg	5.1 ± 0.15%	28	36	47	< 500

[a] The magnesium compositions are given as percentages and not in units of p.p.m.

3. Experimental results

An evaluation of the $\{2\,2\,2\}$ integral peak width ds, of the different alloys as a function of the equivalent deformation ratio, $\bar{\varepsilon}$, is given in Fig. 1. Notice that with an increase in the magnesium amount, the diffraction peaks widen: with no plastic deformation, these differences can be explained by the aluminium- and magnesium-atom size misfit, and the resulting elastic distortion is induced by large magnesium atoms in substitutional positions on the aluminium f.c.c. lattice. On the other hand, in deformed specimens, the higher the amount of magnesium, the higher is the diffraction-profile-peak width, which indicates a higher structural defect density in the materials.

Last, for each alloy, the peak width increases for low deformation ratios, and it reaches a maximum value, d$s_{\max}$, and then it decreases or stabilizes. The value of d$s_{\max}$ increases as the amount of magnesium in the alloys increases, and ranges for equivalent deformation ratios between $\bar{\varepsilon} = 0.3$ and 1.5.

Fig. 2 exhibits the evolution of the distortion factor, ε_1, as a function of the equivalent deformation ratio, $\bar{\varepsilon}$. A similar evolution is observed to the ds evolution, with a rapid increase in ε_1 for low values of the deformation ratio, $\bar{\varepsilon}$, up to a maximum value, after that ε_1 tends towards a stabilization level or it slightly decreases. Compared with aluminium–magnesium alloys, pure aluminium leads to the same-shaped curve, but the absolute value of ε_1 is much smaller. The calculated values of the average coherent domain size, D, show a minimum value increasing $\bar{\varepsilon}$ (Fig. 3). The coherent domain sizes, D, are about 20 nm for aluminium–magnesium alloys and about 80 nm for pure aluminium.

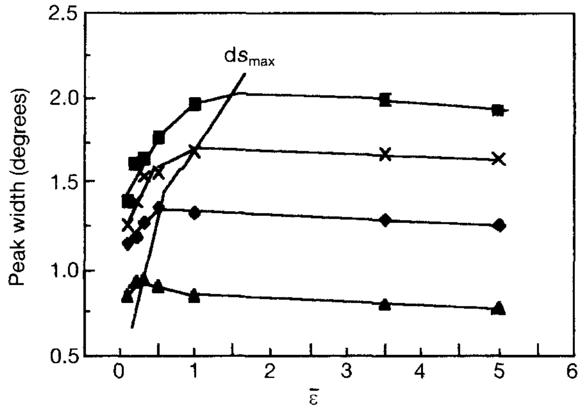

Figure 1 The $\{2\,2\,2\}$ peak width, ds, versus the equivalent deformation ratio, $\bar{\varepsilon}$, for: (◆) Al–1% Mg, (×) Al–3% Mg, (■) Al–5% Mg, and (▲) pure Al.

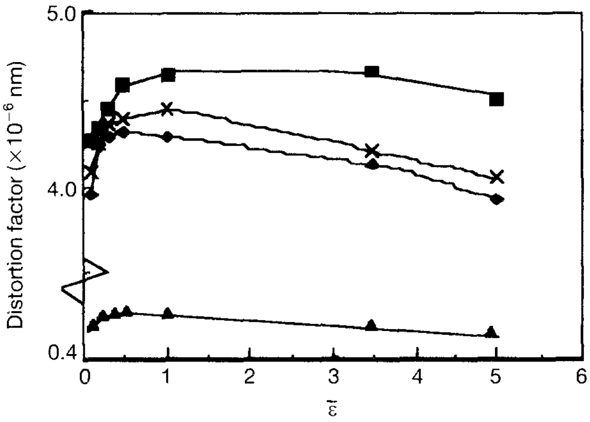

Figure 2 The distortion factor, ε_1, and the equivalent deformation ratio, $\bar{\varepsilon}$, for: (◆) Al–1% Mg, (×) Al–3% Mg, (■) Al–5% Mg, and (▲) pure Al.

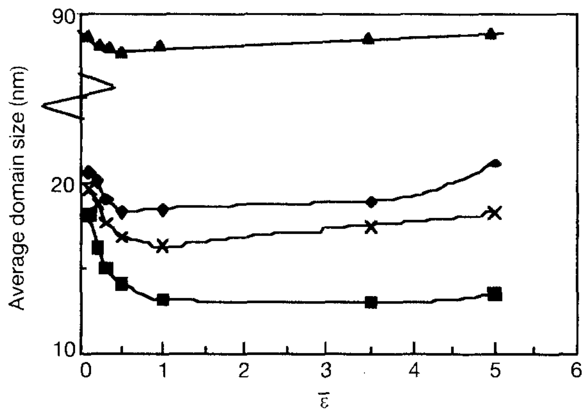

Figure 3 The evolution of the average coherent domain size, *D*, versus $\bar{\varepsilon}$ for: (◆) Al–1% Mg, (×) Al–3% Mg, (■) Al–5% Mg, and (▲) pure Al.

TABLE II The evaluated dislocation densities for the alloys studied; $L = 10$ nm.

$\bar{\varepsilon}$	ρ ($\times 10^{-10}$ cm^{-2})			
	Pure Al	Al-1% Mg	Al-3% Mg	Al-5% Mg
0.1	0.166	2.814	2.857	2.922
0.2	0.218	2.912	2.915	2.950
0.3	0.232	2.929	2.963	2.980
0.5	0.208	2.939	2.963	3.027
1.0	0.180	2.929	3.013	3.046
3.5	0.168	2.874	2.902	3.085
5.0	0.136	2.804	2.804	2.953

From these results, the Williamson–Smallman model [16] allows calculation of an average dislocation density in the materials studied as a function of their plastic deformation. The dislocation density is obtained from [3] using the coherent domain size and the average distortion factor (Table 2):

$$\rho_{av} = c\langle \varepsilon_L^2 \rangle^{1/2}/(Db) \qquad (3)$$

where ***b*** is the Burgers vector, *c* is a dislocation distribution parameter (equal to about 12 in an f.c.c. lattice) and *L* is the total column length over which the internal elastic distortions are averaged. The principle of this calculation was proposed in a very simple way in the 1950s. Recent developments have been proposed for applications in the case of plastic deformation and in the damage studies of materials [17, 18].

As already observed for d*s*, the calculated dislocation density of all the materials depends on the equivalent-plastic-deformation ratio, $\bar{\varepsilon}$, and increases up to a maximum value before it decreases or saturates. From these data, we notice that the calculated dislocation density in the aluminium–magnesium alloys is about one order of magnitude greater than in the pure aluminium. This evolution is found again with the stored energy calculated from the Stibitz expression [19]

$$W_{hkl} = \frac{1.5(E_{hkl})\langle \varepsilon_L^2 \rangle}{1 + 2\gamma_{hkl}^2} \qquad (4)$$

which leads to a value of about 0.05 J g^{-1} for pure aluminium and about 0.5 J g^{-1} for aluminium–magnesium alloys.

4. Discussion

The increases in the integral diffraction peak width, d*s*, the stored energy W_{111} and the dislocation density, ρ_{av}, with the increase in the magnesium addition in the alloys studied are in accordance with a magnesium atom effect in the aluminium matrix and with the evolution of strengthening sensibility effect by work hardening of aluminium alloys with magnesium additions. However the stored energy and dislocation density values, calculated from the XRD-profile-analysis parameters, are lower – by one or two orders of magnitude – than those obtained by direct measurement [13, 14, 20, 21].

On the other hand, the values of ρ_{av}, ε_1 and *D*, have been observed to increase to a maximum value when $\bar{\varepsilon}$ is increased. For each alloy, we observed an extreme value of d*s*, ε_1 and *D* which induced a decrease in *W* and ρ_{av} for a large equivalent deformation ratio, $\bar{\varepsilon}$, even though a continuous increase with deformation was expected. A finer interpretation for these XRD results may be drawn from the results of Thang and Louchet [13, 14] obtained by TEM and by mechanical property measurements. These authors have clearly shown two stages of variation in the plastic deformation mechanism for the alloys.

The first stage for equivalent deformations lower than $\bar{\varepsilon}_0$ (defined by Thang) corresponds to progressive and homogeneous dislocation multiplications which lead to an increase in the stored energy, *W*, and the dislocation density, ρ_{av}, and to a continuous formation of dislocation cells. Those cells were completely structured at $\bar{\varepsilon} = \bar{\varepsilon}_0$.

These values of $\bar{\varepsilon}_0$ increase with the total magnesium atom amount in the alloys and are in excellent agreement with the plastic deformation which leads to the extreme values of d*s*, ε_1 and *D*, as measured by XRD. As a consequence, and for this regime of cold working, the coherent domain size must, therefore, be in close relationship with the mean distance between dislocations in the direction investigated. The average distortion factor is correlated, on the other hand, with the elastic distortion field induced by the dislocation arrangement [15, 22].

Beyond $\bar{\varepsilon}_0$, for large deformation, XRD results indicate an increase in D and a decrease in ε_1 or ds. On the other hand, the TEM results and also the stored-energy evaluation after plastic deformation, which were carried out by Thang [14], show that:

(i) with the increase in $\bar{\varepsilon}$, a stable dislocation cell structure is observed with a progressive but slow decrease in the dislocation cell size;
(ii) new dislocations appear inside the dislocation cells, and they contribute to the wall formation of the dislocation cells; and
(iii) increasing annihilation of dislocations inside the walls, and an increasing rate of dislocation rearrangement in the cells, is observed, and the magnesium additions reduce these evolutions.

In this second stage of deformation, dislocations inside the cells are presumed to have a preponderant effect on the broadening of XRD profiles [8–11, 22], although the dislocations in the walls are the major part of the total dislocation density and they may contribute to the diffraction-profile broadening. As a matter of fact, the mean dislocation cell size (from 0.25 to 5 μm for the corresponding deformation ratio) is not compatible with the diffraction coherent domain size investigated in this work, and it cannot have a direct effect on the XRD-profile broadening; the walls are not compatible either.

The evolution of the calculated values of ds, ε_1 and D seems to be the result, therefore, of the dislocation rearrangement inside the cells. As a matter of fact, the observed progressive decrease in the distortion factor, ε_1, is representative of a dislocation reorganization which allows minimization of the internal lattice elastic distortions of the materials and limits the effective total stored energy in the alloy during the plastic deformation. This dislocation rearrangement leads also to a progressive increase in the average coherent domain size as calculated by diffraction-profile analysis and from the slopes of D–$\bar{\varepsilon}$ and ε_1–$\bar{\varepsilon}$; it was found that the dislocation organization rate inside the cell walls decreased with the magnesium content of the alloys.

This aspect explains the evolution of the underestimated dislocation density and the stored energy from the profile-analysis parameters.

Finally, this analysis is restricted to the evolution of dislocations inside cells and it leads to an underestimated total density of dislocation and the stored energy. The disagreement between the present calculation (derived from XRD-profile analysis) and previous direct measurement is therefore assumed to fit with the dislocation density inside the walls.

5. Conclusions

1. The broadened XRD-profile analysis performed on a commercial pure aluminium and three aluminium–magnesium alloys has been shown to be a valuable and reliable technique for characterizing the microstructural evolution of these materials when they undergo plastic deformations.

2. The XRD-profile-analysis results, D and ε_1, may be used to describe the dislocation structure evolution of materials during plastic deformation. Two stages have been identified as a function of the applied equivalent deformation ratio, $\bar{\varepsilon}$, and they are in very good agreement with direct observations performed by TEM.

(a) $-\ \bar{\varepsilon} < \bar{\varepsilon}_0$ (small deformation, low cold working), a stage of homogeneous dislocation multiplication leading to an effective increase in the dislocation densities, ρ, and stored energies, W, in the material, in relation to the plastic deformation and magnesium additions.
(b) $-\ \bar{\varepsilon} > \bar{\varepsilon}_0$ (large deformation, large cold working), a stage of cellular-dislocation substructure development for which the diffraction-profile analysis indicates a dislocation rearrangement inside the cells as a function of the equivalent deformation level and the magnesium additions.

For stage (b), the dislocations visible by XRD are only 1/10 of the total dislocation density; the cell walls are not seen. The evolution of the XRD-profile-analysis parameters (ds, D) and evaluated dislocation density ρ_{av} seems to be an indicator of dislocation rearrangement inside the cells for stage (b) of the deformation after a previous evolution leading to cell formation.

Acknowledgements

The authors are grateful to O. Leneel for his technical help and to Dr G. M. Raynaud for providing the specimens studied.

References

1. J. D. EMBURY, A. KELLY and R. NICHOLSON, "Strengthening methods in crystals" (Applied Science, New York, 1971) p. 331.
2. LIU YI-LIN, L. DELAEY, E. AERNOUDT and O. ARKENS, *Mater. Sci. Engng.* **96** (1987) 125.
3. BENT BAY and NIELS HANSEN, Second RISO International Symposium on Metallurgy and Material Science, Nenwark, Denmark, edited by N. Hansen, A. Horsewell, T. Leffers and H. Liholt (RISO National Laboratory, 1981) p. 137.
4. D. J. LLOYD and D. KENNY, *Metall. Trans. A* **13** (1982) 1445.
5. BENT BAY and NIELS HANSEN, *ibid.* **15** (1984) 287.
6. MARIE RICHERT, *Z. Metallkde.* **78** (1987) 862.
7. B. E. WARREN, "X-ray diffraction" (Addison-Wesley, London, 1969).
8. M. WILKENS, *Phys. Status Solidi* (*a*) **2** (1970) 359.
9. B. BOURNIQUEL, J. M. SPRAUEL, J. FERON and J. L. LEBRUN, Symposium of Second International Conference on residual stresses, Nancy, France, edited by G. Beck, S. Denis and A. Simon (Elsevier Applied Science, London, 1989) p. 184.
10 N. JI, J. L. LEBRUN, P. BELLIARD, B. BOURNIQUEL and G. MAEDER, *ibid.* p. 65.
11. T. UNGAR, H. MUGHRABI and M. WILKENS, Fifth RISO International Symposium on Metallurgy and Material Science, Rooklide, Denmark, edited by N. H. Andersen, M. Eldrup, N. Hansen, D. Juul Jensen, T. Leffers, H. Lulholt, O. B. Pedersen and B. N. Singh (RISO National Laboratory, 1984) p. 539.
12. Y. M. WANG, S. S. LEE and Y. C. LEE, *J. Appl. Cryst.* **15** (1982) p. 35.

13. T. Q. THANG, PhD thesis, Institute National Polytechnique de Grenoble, Grenoble, France, 1986.
14. F. LOUCHET and T. Q. THANG, Symposium of Colloque Plasticity 88, Grenoble, March 1988.
15. N. JI, J. L. LEBRUN and J. BONNIN, *J. Mater. Sci. Lett.* **8** (1989) 1127.
16. G. K. WILLIAMSON and R. E. SMALLMAN, *Phil. Mag.* **1** (1956) 34.
17. I. R. KRAMER, B. WU and C. R. FENG, *Mater. Sci. Engng.* **82** (1986) 141.
18. I. C. NOYAN and J. B. COHEN, *ibid.* **75** (1985) 179.
19. G. R. STIBITZ, *Phys. Rev.* **49** (1936) 862.
20. R. E. SMALLMAN, "Modern physical metallurgy", (Butterworths, London, 1970).
21. M. B. BEVER, D. L. HOLT and A. L. TITCHENER, "The stored energy of cold work" (Pergamon Press, Oxford, 1973).
22. N. JI, PhD thesis, Ecole Nationale Superieure d'Arts et Métiers, Paris, France (1989).

Received 26 October 1992
and accepted 9 September 1993